Received: 27 December 2021 | Revised: 21 February 2022 | Accepted: 26 February 2022

DOI: 10.1002/lio2.771

ORIGINAL RESEARCH

Laryngoscope Investigative Otolaryngology

Downregulation of circLPAR3 inhibits tumor progression and glycolysis by liberating miR-144-3p and upregulating LPCAT1 in oral squamous cell carcinoma

Zhijian Su MM | Chao Pan MM | Honghui Xie MM | Yanyang Ning MM | Shuangjiang Li MM | Haibo Xiao MM

Department of Endodontics, Changsha Stomatological Hospital, Changsha, China

Correspondence
Haibo Xiao, Department of Endodontics, Changsha Stomatological Hospital, No. 389, Youyi Road, Tianxin District, Changsha 410008, China.
Email: xiaohaibo2021@126.com

Abstract

Background: Increasing evidence demonstrated the important roles of circular RNAs (circRNAs) in human cancer progression, including oral squamous cell carcinoma (OSCC). The study intentions were to explore the role and molecular mechanism of hsa_circ_0004390 (circLPAR3) in OSCC progression.

Methods: Expression of circLPAR3 in collected samples and cultured cell lines was detected with real-time quantitative reverse transcription-polymerase chain reaction (RT-qPCR). Loss-of-function experiments were performed to determine the effect of circLPAR3 silencing on OSCC cell proliferation, migration, invasion, apoptosis, angiopoiesis, and glycolysis. The sponge function of circLPAR3 was predicted by bioinformatics analysis and validated by the dual-luciferase reporter and RNA pull-down assays. In vivo experiments were conducted to validate the function of circLPAR3.

Results: A marked increase in circLPAR3 expression was observed in OSCC samples and cell lines. Furthermore, circLPAR3 could distinguish OSCC samples from paired non-tumor samples, and patients with high circLPAR3 expression had a poor prognosis. Furthermore, circLPAR3 inhibition decreased OSCC growth in xenograft mouse models. Moreover, circLPAR3 silencing repressed cell proliferation, migration, invasion, angiopoiesis, glycolysis, and induced cell apoptosis in OSCC cells in vitro. Mechanically, circLPAR3 sponged miR-144-3p to prohibit the inhibiting effect of miR-144-3p on LPCAT1, thus promoting OSCC progression.

Conclusion: CircLPAR3 exerted a tumor-promoting effect on OSCC growth through elevating LPCAT1 expression via functioning as a miR-144-3p sponge. This study supports the possible role of circLPAR3 in the diagnosis, prognosis, and treatment of OSCC.

KEYWORDS
circLPAR3, LPCAT1, miR-144-3p, OSCC

1 | INTRODUCTION

Oral squamous cell carcinoma (OSCC) accounts for more than 90% of all oral malignancies, with a 5-year survival rate under 50%.[1] Surgery combined with immune checkpoint inhibitors, chemotherapy, and radiotherapy is the main treatment strategy for OSCC.[2] Studies have shown that up to 40% of patients have disease recurrence within 2 years after treatment.[3,4] Therefore, understanding the advancement of OSCC at the molecular level is indispensable for discovering new therapeutic targets for this disease.

Circular RNAs (circRNAs) differ from their linear RNA forms in that they form a closed-loop structure through a reverse splicing mechanism.[5] Their annular structure makes them more stable and exhibits a longer half-life than their respective linear RNAs.[6] In the beginning, circRNAs were thought to deal with errors in the RNA splicing mechanism.[7] According to recent research, circRNAs may be involved in many biological processes and may be key regulators of many aspects of cell and tissue homeostasis.[8] More and more research has displayed the vital roles of circRNAs in tumorigenesis and advancement, including OSCC.[9] For instance, circ-102,450 exerts a repressive effect on OSCC cell invasion and proliferation.[10] Also, circ-IGHG[11] and circ-EPSTI1[12] contribute to OSCC progression through inducing epithelial-to-mesenchymal transition.

One of the main mechanisms underlying the regulatory action of circRNAs is related to the ability of these molecules to act as microRNA (miRNA) sponges.[13,14] That is, circRNAs, as competing for endogenous RNAs (ceRNAs), compete with mRNA to share miRNAs, thereby regulating gene expression.[15] Multiple lines of evidence have uncovered the deregulation of the circRNA/miRNA/mRNA axis during OSCC development. Also, circ-FOXO3 sequesters miR-214 and subsequently causes the upregulation of KDM2A, thus promoting the progression of OSCC.[16] Furthermore, circ-SEPT9 increases PKN2 expression through adsorbing miR-1225, thus facilitating OSCC advancement.[17] Therefore, expanding the knowledge of circRNAs regulating the complex ceRNA network in OSCC will help solve problems related to the pathogenesis and treatment of these diseases.

Hsa_circ_0004390 (circLPAR3), located at chr1: 85331067–85,331,821, is overexpressed in the circRNA expression profile in OSCC samples.[18] A recent report suggested the oncogenic role of circLPAR3 in OSCC,[19] but the role of circLPAR3 and its function as a miRNA sponge needs to be further explored.

2 | MATERIALS AND METHODS

2.1 | Patient specimens

A total of 82 samples, including 41 OSCC samples and 41 corresponding non-tumor samples, were obtained at the Changsha Stomatological Hospital. The written consents were signed by these participants. The Ethics Committee of Changsha Stomatological Hospital consented to this experiment.

2.2 | Cell culture

The HOK cell line (Sciencell) was cultured in Oral Keratinocyte Medium (ScienCell). Three cell lines SCC9, SCC4, and SCC25 were obtained from (ATCC) and maintained in a 1:1 mixture of Dulbecco's modified Eagle's medium (DMEM) and Ham's F12 medium (ATCC) supplemented with 400 ng/ml hydrocortisone [Sigma–Aldrich (SA)], 10% fetal bovine serum (Thermo), and 1% penicillin–streptomycin (SA). Three cell lines UM1 (JCRB), HSC3 (JCRB), and CAL27 (ATCC) were maintained in DMEM (ATCC) supplemented with 10% fetal bovine serum (Thermo) and 1% penicillin–streptomycin (SA). The growth environment of these cells was in an incubator set at 37°C with 5% carbon dioxide.

2.3 | RNA preparation, complementary DNA synthesis, and real-time quantitative polymerase chain reaction (RT-qPCR)

Extraction of total RNA from collected samples and cultured cells was carried out using the RiboEx TM (GeneAll®) as per the manufacturer's instructions. Fractionation of nuclear RNA and cytoplasmic RNA from cultured cells was conducted using the active motif's nuclear extract kit. Following the evaluation of quantity and quality, the extracted RNA was reverse transcribed using the PrimeScript™ 1st Strand cDNA Synthesis Kit (Takara) (for circRNA and mRNA) or miRCURY LNA™ Universal RT miRNA PCR system (Exiqon) (for miRNA). Expression levels were measured in triplicate with a RealQ Plus 2× Master Mix Green (low Rox) (Ampliqon) on the Lightcycler 96 (Roche). Relative fold change was evaluated using Equation $2^{-\Delta\Delta Ct}$ with GAPDH and U6 as the reference genes. Primer sequences were listed in Table 1.

TABLE 1 Primer sequences used for RT-qPCR

Genes	Primer sequences (5′–3′)
circLPAR3	Forward (F): 5′-CAACGTCTTGTCTCCGCATA-3′
	Reverse (R): 5′-CGACAGTATCAGTGTTGCTCCT-3′
LPAR3	F: 5′-GAACGTGAGCGGATGTTCA-3′
	R: 5′-AGGCAGAAAAACGTCCCAAC-3′
miR-144-3p	F: 5′-GCGCGCGTACAGTATAGATGA-3′
	R: 5′-AGTGCAGGGTCCGAGGTATT-3′
LPCAT1	F: 5′-CACAACCAAGTGGAAATCGAG-3′
	R: 5′-GCACGTTGCTGGCATACA-3′
β-Actin	F: 5′-TGGATCAGCAAGCAGGAGTA-3′
	R: 5′-TCGGCCACATTGTGAACTTT-3′
U6	F: 5′-CTCGCTTCGGCAGCACATA-3′
	R: 5′-CGAATTTGCGTGTCATCCT-3′

2.4 | Actinomycin D and RNase R assays

OSCC cells were grown in a complete medium supplemented with actinomycin D (100 ng/ml, CST) (a transcription inhibitor) to evaluate the stability of circLPAR3. OSCC cells-derived total RNA (5 μg) was digested with or without RNase R (Lucigen) at 70°C for 10 min to validate the circular structure of circLPAR3. Following actinomycin D treatment, the total RNA was isolated using the RiboEx TM (GeneAll®). Following RNase R digestion, RNA samples were purified with the Direct-zolTM kit (Zymo Research). The obtained RNA samples were subjected to RT-qPCR analysis.

2.5 | Lentiviral transduction of target cells

The lentivirus carrying a short hairpin RNA against circLPAR3 (sh-circLPAR3#1, sh-circLPAR3#2, or sh-circLPAR3#3) was generated using the pLKO.1 vector (Addgene) with sh-NC as a control. To generate lentiviral particles, HEK-293T cells were seeded on 10 cm plates and co-transected with the lentivirus packaging system (PAX2 and pMD2.G) and a recombinant lentiviral plasmid using GeneJuice® transfection reagent (Millipore). The produced lentiviral particles were added to the culture of target SCC25 and HSC3 cells. Puromycin selection was performed 72 hr after transduction to select available cells.

2.6 | Plasmids, miRNA mimic, and miRNA inhibitor

Generation of the LPCAT1 overexpression plasmid was performed by inserting the full-length LPCAT1 cDNA into the pcDNA3.1 (+) vector (Thermo) at EcoRI and NotI sites. MiR-144-3p inhibitor and mimic synthesized by (Ribobio) were utilized to overexpress and knock down miR-144-3p, and in-miR-NC or miR-NC was used as controls. Transfection was carried out using TransIT-X2 (Mirus Bio.).

2.7 | Clonogenic assay

A single-cell suspension with a specific number (1×10^3 cells/well) was grown on 6-well plates for 10 days. Following washing with PBS (Thermo), the colonies were stained with 0.25% crystal violet (SA). The colonies (more than 50 cells) were captured and counted using an IX71 fluorescence microscope (Olympus).

2.8 | 5-ethynyl-2′-deoxyuridine (EdU) incorporation assay

In brief, about 2×10^4 OSCC cells were cultured using the EdU Imaging Detection Kit (KeyGEN) as per the manufacturer's instructions. Nuclei were then labeled with blue fluorescence (DAPI), and the

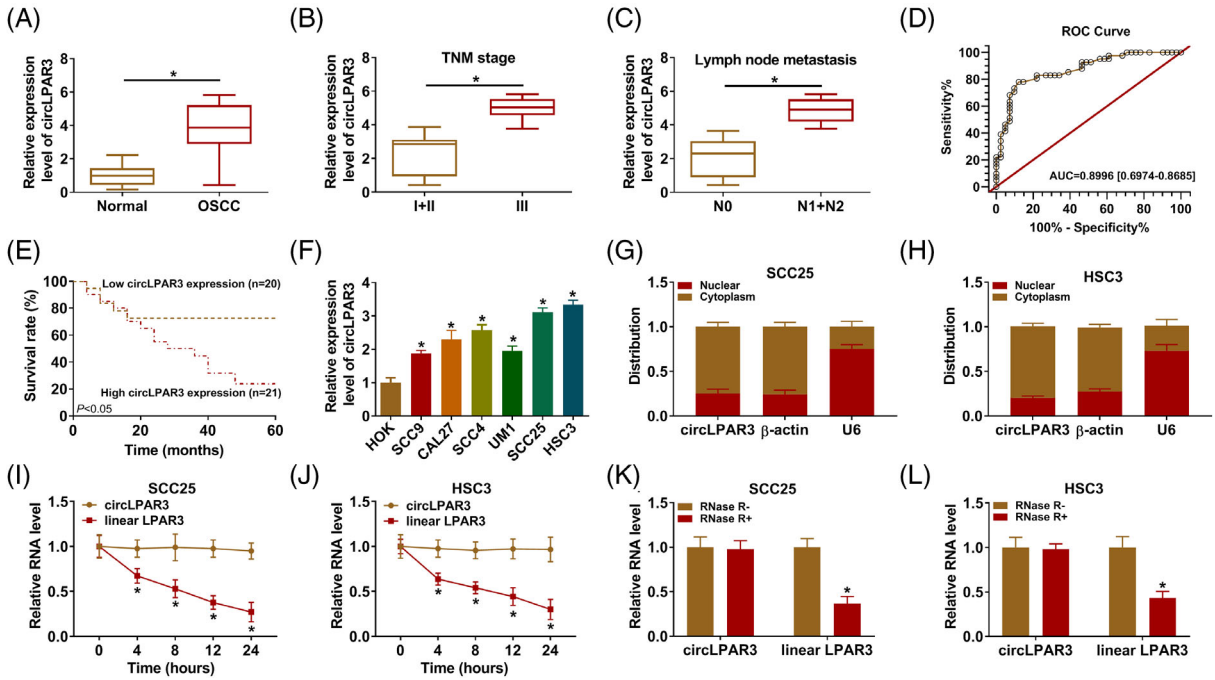

FIGURE 1 CircLPAR3 was highly expressed in OSCC. (A–C) RT-qPCR analysis of circLPAR3 expression in OSCC samples (compared to marching non-tumor samples), OSCC samples in stage III (compared to OSCC samples in stage I + II), and OSCC samples in N1 + N2 stages (compared to OSCC samples in the N0 stage). (D) ROC analysis assessment of the diagnosis value of circLPAR3. (E) Kaplan–Meier analysis evaluation of the value of circLPAR3 as a biomarker of prognosis. (F) RT-qPCR analysis of circLPAR3 expression in OSCC cell lines (compared to the HOK cell line). (G and H) The proportion of circLPAR3 in the cytoplasmic RNA and nuclear RNA of SCC25 and HSC3 cells. (I and J) Actinomycin D assay analysis of the stability of circLPAR3. (K and L) RNase R assay evaluation of the circular structure of circLPAR3. *$p < .05$

positive cells were analyzed Image-Pro Plus 6.0 Software (Media Cybernetics) after taking pictures with a fluorescence microscope (Olympus).

2.9 | Transwell assay

Transwell inserts coated with Matrigel were used to analyze invasion, and transwell inserts without Matrigel were used to analyze migration. Analysis of cell migration and invasion was performed as previously described.[20] Cells were counted using an inverted microscope (Olympus).

2.10 | Western blotting

Total protein was extracted using RIPA lysis buffer with protease and phosphates inhibitor (SA). 20 μg protein extracts were loaded onto each well of 10% SDS-PAGE. Separated proteins were then transferred onto a PVDF membrane (Millipore). Following blocking with 5% skim milk powder, the membrane was probed with primary antibodies against PCNA at 1:1000 dilution (ab92552, Abcam), E-cadherin at 1:10,000 dilution (ab40772, Abcam), Vimentin at 1:1000 dilution (ab92547, Abcam), Bax at 1:1000 dilution (ab32503, Abcam), Bcl-2 at 1:1000 dilution (ab32124, Abcam), LPCAT1 at 1:1000 dilution (ab166903, Abcam), and β-actin at a concentration of 1 μg/ml (ab8224, Abcam). Membranes were then incubated with an appropriate secondary antibody (Abcam). Protein bands were viewed using an enhanced chemiluminescence detection system with a chemiluminescence HRP Substrate (Millipore).

2.11 | Tube formation assay

HUVECs were seeded on Matrigel-coated 24-well plates and incubated with conditioned medium derived from OSCC cells for 6 hr.

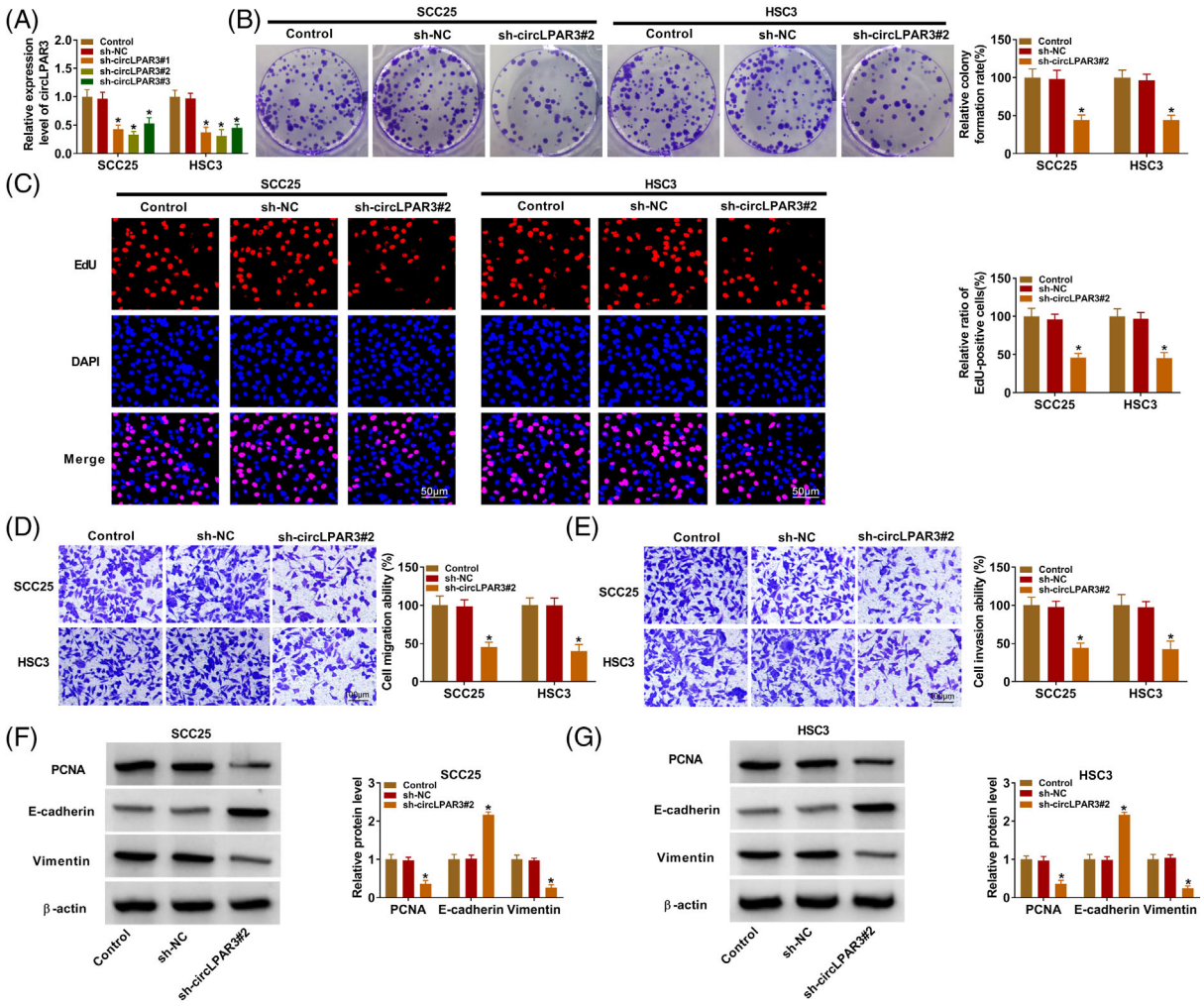

FIGURE 2 CircLPAR3 silencing repressed OSCC cell proliferation, migration, and invasion. (A) The interference efficiencies of sh-circLPAR3#1, sh-circLPAR3#2, and sh-circLPAR3#3 were validated. (B–E) The proliferation, migration, and invasion of control cells and OSCC cells with sh-NC or sh-circLPAR3#2 were analyzed by clonogenic, EdU, and transwell assays. (F and G) Western blotting analysis of the protein levels of PCNA, E-cadherin, and Vimentin in the above cells. *$p < .05$

Tube formation was quantified with Image-Pro Plus 6.0 Software (Media Cybernetics) after taking pictures with a microscope (Olympus).

2.12 | Flow cytometry assay

The single-cell suspension with a specific number (3×10^5 cells/well) was stained with the Annexin V-FITC/PI kit (KeyGEN) according to the producer's guidelines. The flow cytometer (Becton Dickinson) was used to detect the cells.

2.13 | Lactate production and glucose consumption

After culturing for 48 hr, the lactate production and glucose consumption of transfected OSCC cells were analyzed with a Glucose Assay Kit (Solarbio, Beijing, China) and Lactate Assay Kit (Solarbio) based on the manufacturer's instructions.

2.14 | Dual-luciferase reporter assay

OSCC cells were co-transfected with pRL-TK, a luciferase reporter, and miR-144-3p mimic or miR-NC using GeneJuice® transfection reagent (Millipore). The luciferase reporters circLPAR3 WT, LPCAT1 3′UTR WT, circLPAR3 MUT, and LPCAT1 3′UTR MUT were constructed using the pmirGLO vector (Promega), respectively. Forty-eight hours later, luciferase activities were measured using the dual-luciferase reporter system (Promega), and Renilla activity was used to normalize firefly activity.

2.15 | RNA pull-down assay with biotinylated circLPAR3 probe

The Bio-NC, Bio-circLPAR3 WT, and Bio-circLPAR3 MUT probes (Tsingke, Wuhan, China) were incubated with streptavidin magnetic beads (Thermo). OSCC cell lysates-derived supernatants were incubated with the magnetic beads obtained in the step above at 4°C

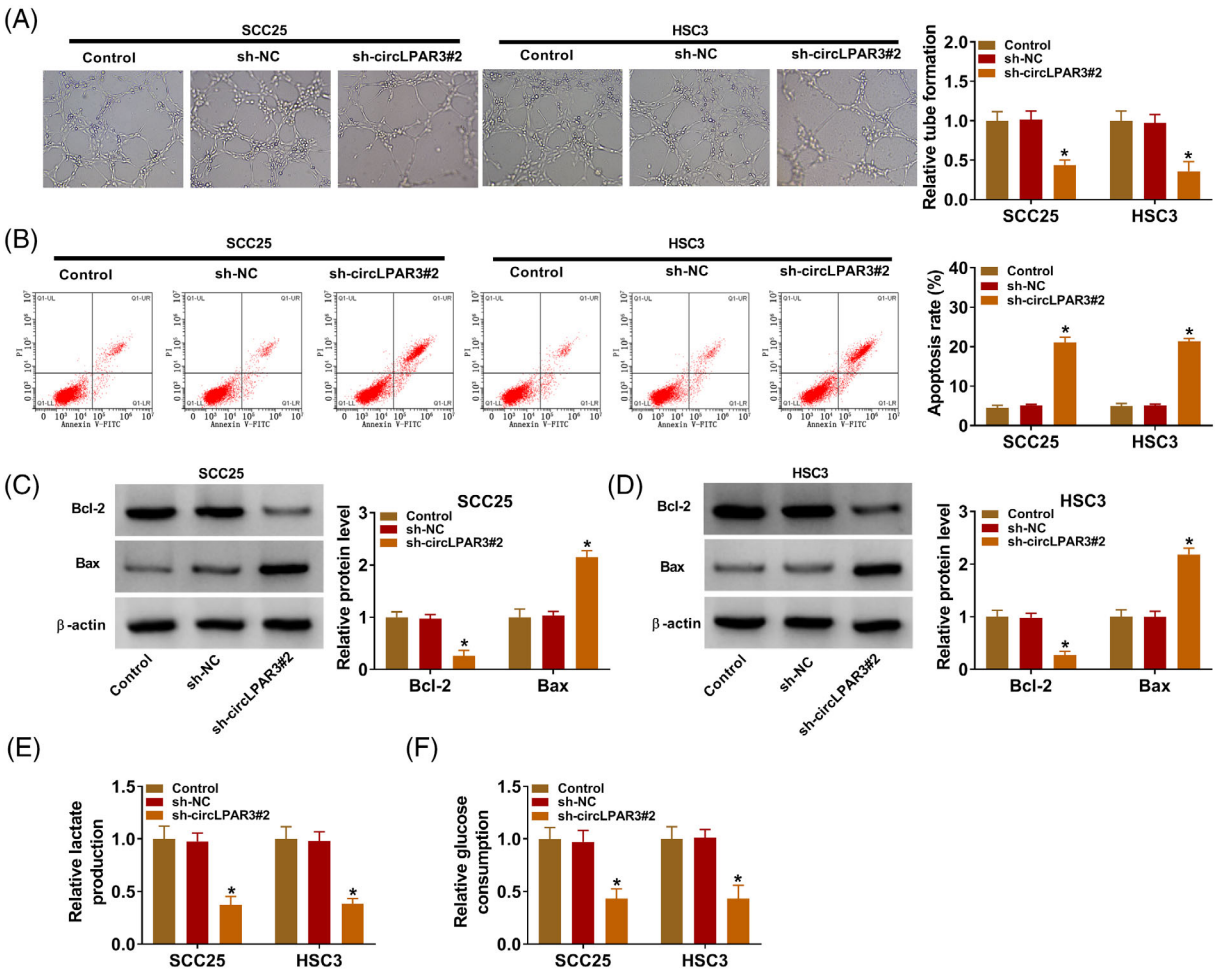

FIGURE 3 CircLPAR3 knockdown restrained angiopoiesis, promoted apoptosis, and decreased glycolysis of OSCC cells. (A and B) The angiopoiesis and apoptosis of control cells and OSCC cells with sh-NC or sh-circLPAR3#2 were assessed by tube formation and flow cytometry assays. (C and D) Protein levels of Bcl-2 and Bax in the above cells. (E and F) Analysis of lactate production and glucose consumption in the above cells. *$p < 0.05$

overnight, and the bound miR-144-3p in RNA complexes were detected with RT-qPCR.

2.16 | RNA pull-down assay with biotinylated miR-144-3p probe

Sonication was performed to treat OSCC cells transfected with Bio-NC, Bio-miR-144-3p WT, or Bio-miR-144-3p MUT (Tsingke). The supernatants were incubated with activated streptavidin beads (Thermo) at 4°C overnight. RNA complexes were subjected to RT-qPCR analysis after elution from streptavidin beads.

2.17 | Xenograft assay

Animal experiments were approved by the Animal Ethics Committee of Changsha Stomatological Hospital. 10 BALB/c male nude mice (4 weeks old, 15–20 g) (Vital River, Beijing, China) were reared at specific pathogen-free condition. For the xenograft assay, SCC25 cells (1×10^7) with sh-circLPAR3#2 or sh-NC were subcutaneously injected into the back of each nude mouse (5 mice per group). Tumor volume was recorded once a week [(length × width^2)/2]. Twenty-eight days later, the mice were sacrificed and their xenograft tumors were stripped. The obtained xenograft tumors were fixed with 4% formaldehyde and then embedded in paraffin. Immunohistochemistry (IHC) analysis was carried out as previously described.[21] Primary antibodies included LPCAT1 (ab166903, Abcam) and PCNA (ab92552, Abcam).

2.18 | Statistical analysis

Results are expressed as the mean ± SD of at least three different experiments performed in triplicate. Data were analyzed using Student's *t*-test or analysis of variance in GraphPad Prism 8 software (GraphPad). Values were considered significantly different if $p < .05$.

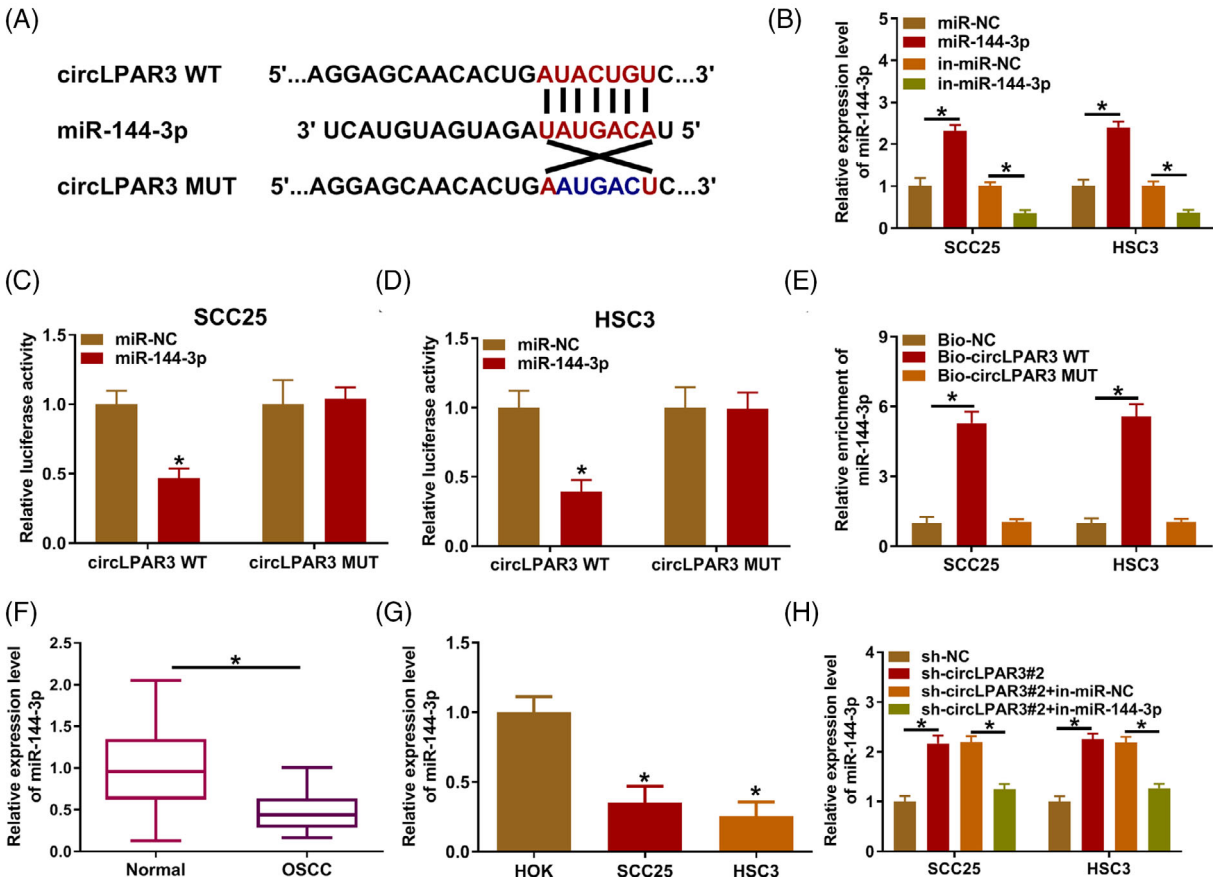

FIGURE 4 The sponge function of circLPAR3 to miR-144-3p was validated. (A) Schematic diagram of the binding sites between circLPAR3 and miR-144-3p. (B) The transfection efficiencies of miR-144-3p mimic (relative to miR-NC) and miR-144-3p inhibitor (relative to in-miR-NC). (C and D) Dual-luciferase reporter assay analysis of the luciferase activity of the circLPAR3 WT or circLPAR3 MUT reporter in miR-144-3p-overexpressing OSCC cells. (E) Enrichment of miR-144-3p by Bio-NC, Bio-circLPAR3 WT, or Bio-circLPAR3 MUT probe was assessed. (F and G) Expression of miR-144-3p in OSCC samples (compared to marching non-tumor samples) and cells (compared to the HOK cell line). (H) Effect of miR-144-3p knockdown on miR-144-3p expression in circLPAR3-knockdown OSCC cells. *$p < .05$

3 | RESULTS

3.1 | CircLPAR3 was highly expressed in OSCC and might become diagnostic and prognostic biomarkers for OSCC

To explore the function of circLPAR3 in OSCC, we analyzed circLPAR3 expression in OSCC samples and cell lines. RT-qPCR showed an overt upregulation of circLPAR3 in OSCC samples when compared to corresponding normal samples (Figure 1A). Moreover, tumor samples in stage III had higher levels of circLPAR3 compared to tumor samples in stage I + II (Figure 1B). Also, higher levels of circLPAR3 were observed in OSCC samples in N1 + N2 stages than those in the N0 stage (Figure 1C). ROC analysis showed the meaningful value of circLPAR3 in distinguishing between OSCC samples and normal samples (AUC = 0.8996) [0.6974–0.8685] (Figure 1D). Kaplan–Meier analysis exhibited a worse prognosis in patients with high circLPAR3 expression (Figure 1E). We also observed that circLPAR3 was overexpressed in OSCC cell lines relative to the HOK cell line, and two OSCC cell lines SCC25 and HSC3 with the highest circLPAR3 level were used for functional analysis (Figure 1F). Nucleplasmic separation assays exhibited that circLPAR3 was distributed in both nucleus and cytoplasm and more localized in the cytoplasm, and the distribution of circPAR3 in SCC25 and HSC3 cells was similar (Figure 1G,H). Actinomycin D and RNase R assays exhibited that circLPAR3 had a longer half-life and anti-RNase R digestion when compared with linear LPAR3 transcript, indicating that the circular PAR3 transcript was more stable (Figure 1I-L). Collectively, these results manifested that circLPAR3 might be associated with OSCC advancement.

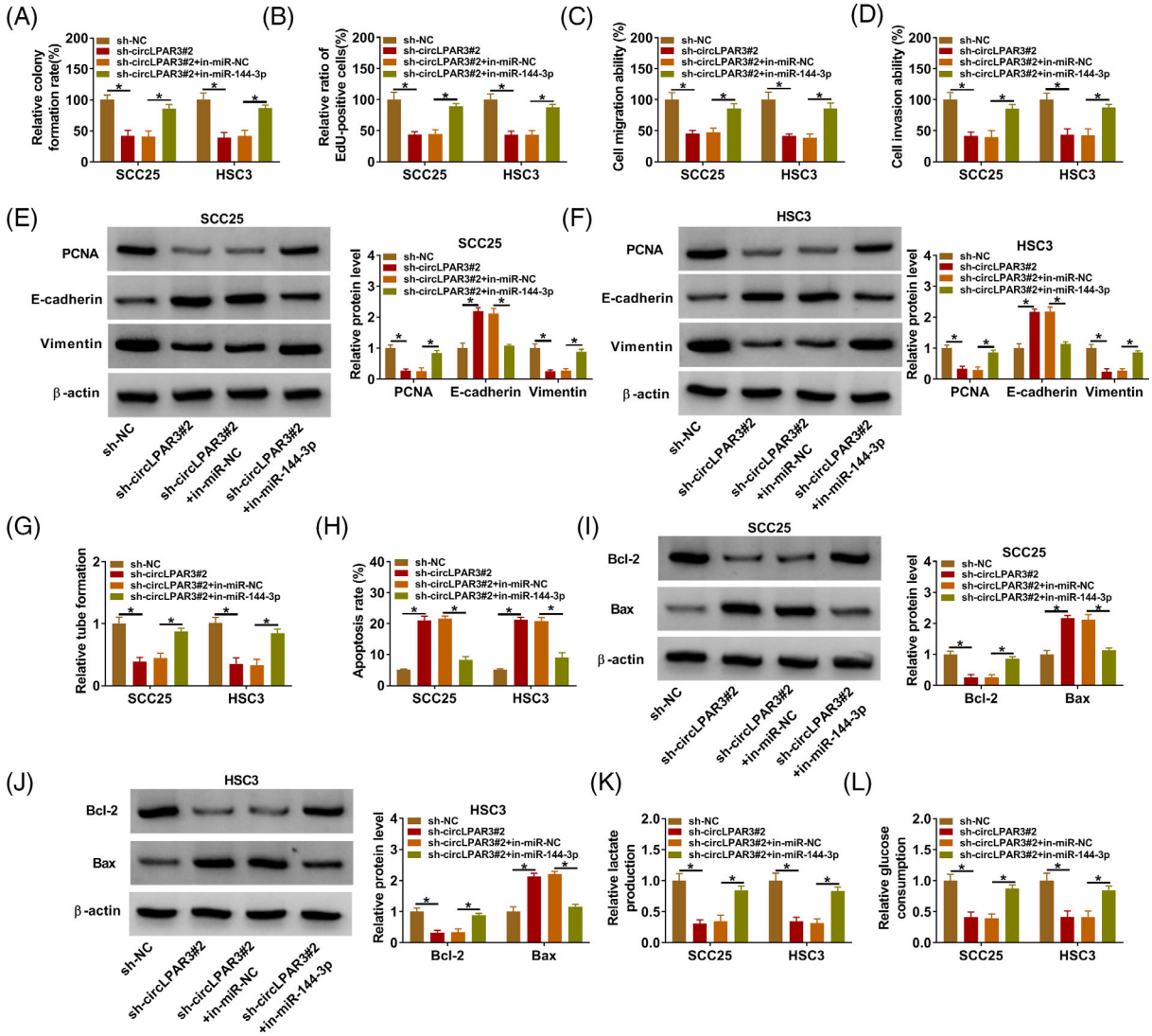

FIGURE 5 CircLPAR3 interacted with miR-144-3p to regulate proliferation, migration, invasion, angiopoiesis, and glycolysis of OSCC cells. (A–D) The proliferation, migration, and invasion of OSCC cells with sh-NC, sh-circLPAR3#2, sh-circLPAR3#2+in-miR-NC, or sh-circLPAR3#2+in-miR-144-3p were analyzed. (E and F) Protein levels of PCNA, E-cadherin, and Vimentin in the above cells were detected. (G and H) The angiopoiesis and apoptosis of the above cells were determined. (I and J) Protein levels of Bcl-2 and Bax in the above cells were analyzed. (K and L) The lactate production and glucose consumption of the above cells. *$p < .05$

3.2 | Inhibition of circLPAR3 reduced OSCC cell proliferation, migration, and invasion

We constructed SCC25 and HSC3 cell lines with stable knockdown of circLPAR3 to further explore the function of circLPAR3. The interference efficiencies of three shRNAs targeting the junction sites of circLPAR3 (sh-circLPAR3#1, sh-circLPAR3#2, and sh-circLPAR3#3) were exhibited in Figure 2A, and sh-circLPAR3#2 caused a lowest circLPAR3 level was used for further analysis. Colony formation and EdU assays exhibited that circLPAR3 knockdown repressed OSCC cell proliferation (Figure 2B,C). Transwell assay showed that the migratory and invade abilities of circLPAR3-knockdown OSCC cells were lower (Figure 2D,E). Also, PCNA and Vimentin protein levels were decreased in circLPAR3-knockdown cells, but E-cadherin protein levels were elevated (Figure 2F,G). Together, these results suggested that circLPAR3 promoted OSCC cell proliferation, migration, and invasion.

3.3 | Silencing of circLPAR3 repressed angiopoiesis, induced apoptosis, and decreased glycolysis in OSCC cells

Further tube formation assays showed that circLPAR3 silencing decreased the number of tube formations (Figure 3A). Cell apoptosis analysis showed that knockdown of circLPAR3 caused more OSCC cell apoptosis (Figure 3B). Moreover, Bax protein levels were elevated and Bcl-2 protein levels were reduced in circLPAR3-inhibiting cells (Figure 3C,D). In addition, there was a marked decrease in lactate production and glucose consumption in circLPAR3-silencing cells (Figure 3E,F). Together, these findings suggested that circLPAR3 promoted angiopoiesis and glycolysis of OSCC cells.

3.4 | CircLPAR3 served as a miR-144-3p sponge

Because circLPAR3 was more localized in the cytoplasm, we further explored the function of circLPAR3 as a miRNA sponge. Circular RNA Interactome prediction showed that circLPAR3 might function as a miR-144-3p sponge (Figure 4A). To test their relationship, miR-144-3p mimic and inhibitor were, respectively, transfected into OSCC cells to overexpress and silence miR-144-3p (Figure 4B). Further luciferase assays exhibited that miR-144-3p overexpression reduced the luciferase activity of the circLPAR3 WT reporter but not the circLPAR3 MUT reporter (Figure 4C,D). Biotin-labeled circLPAR3 probing showed that circLPAR3 was significantly pulled down by the Bio-circLPAR3 WT probe instead of the Bio-circLPAR3 MUT probe (Figure 4E). Also, miR-144-3p was underexpressed in OSCC samples and cell lines (Figure 4F, G). Co-administration of miR-144-3p inhibitor and sh-circLPAR3

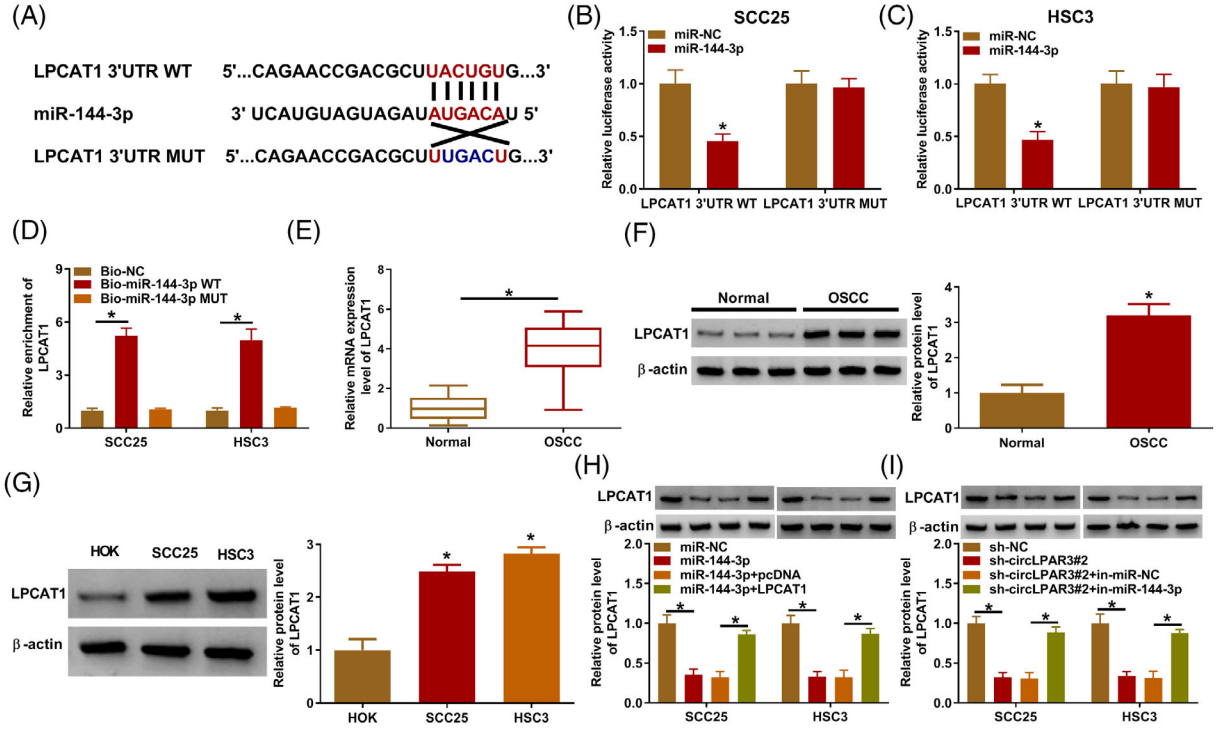

FIGURE 6 LPCAT1 acted as a miR-144-3p target. (A) Schematic diagram of the binding sites between LPCAT1 and miR-144-3p. (B and C) Dual-luciferase reporter assay evaluation of the luciferase activity of the LPCAT1 3′UTR WT or LPCAT1 3′UTR MUT reporter in miR-144-3p-overexpressing OSCC cells. (D) The enrichment of LPCAT1 in the Bio-NC, Bio-miR-144-3p WT, or Bio-miR-144-3p MUT group. (E and F) The mRNA and protein levels of LPCAT1 in OSCC samples (compared to marching non-tumor samples). (G) The levels of LPCAT1 protein in OSCC cells (compared to the HOK cell line). (H) Effect of LPCAT1 overexpression inhibition on LPCAT1 protein levels in miR-144-3p-overexpressing OSCC cells. (I) Impact of miR-144-3p knockdown on LPCAT1 protein levels in circLPAR3-knockdown OSCC cells. *$p < .05$

impaired the increase in miR-144-3p expression in OSCC cells caused by sh-circLPAR3 alone (Figure 4H). Collectively, these results manifested that circLPAR3 acted as a miR-144-3p sponge.

3.5 | CircLPAR3 regulated proliferation, migration, invasion, angiopoiesis, and glycolysis of OSCC cells through interaction with miR-144-3p

To identify whether circLPAR3 interacts with miR-144-3p to mediate OSCC cell proliferation, migration, invasion, angiopoiesis, and glycolysis, rescue experiments were performed. CircLPAR3 silencing-mediated repression on OSCC cell proliferation, migration, and invasion was mitigated after co-transfection with miR-144-3p inhibitor (Figure 5A–D). The changes of PCNA, E-cadherin, and Vimentin protein levels in circLPAR3-inhibiting cells were partly reversed after miR-144-3p knockdown (Figure 5E,F). The silencing of miR-144-3p overturned the reduction in tube formation and the elevation in apoptosis in OSCC cells prompted by circLPAR3 knockdown (Figure 5G,H). Also, the impacts of circLPAR3 inhibition on Bcl-2 and Bax protein levels were reversed by miR-144-3p silencing (Figure 5I,J). Furthermore, the reduced lactate production and glucose consumption in circLPAR3-knockdown cells were weakened after miR-144-3p inhibitor introduction (Figure 5K,L). Collectively, these results exhibited that circLPAR3 regulated proliferation, migration, invasion, angiopoiesis, and glycolysis of OSCC cells via interaction with miR-144-3p.

3.6 | LPCAT1 was a miR-144-3p target

To explore the molecular mechanism by which miR-144-3p mediates OSCC cell malignant behaviors, bioinformatics analysis (starbase) was

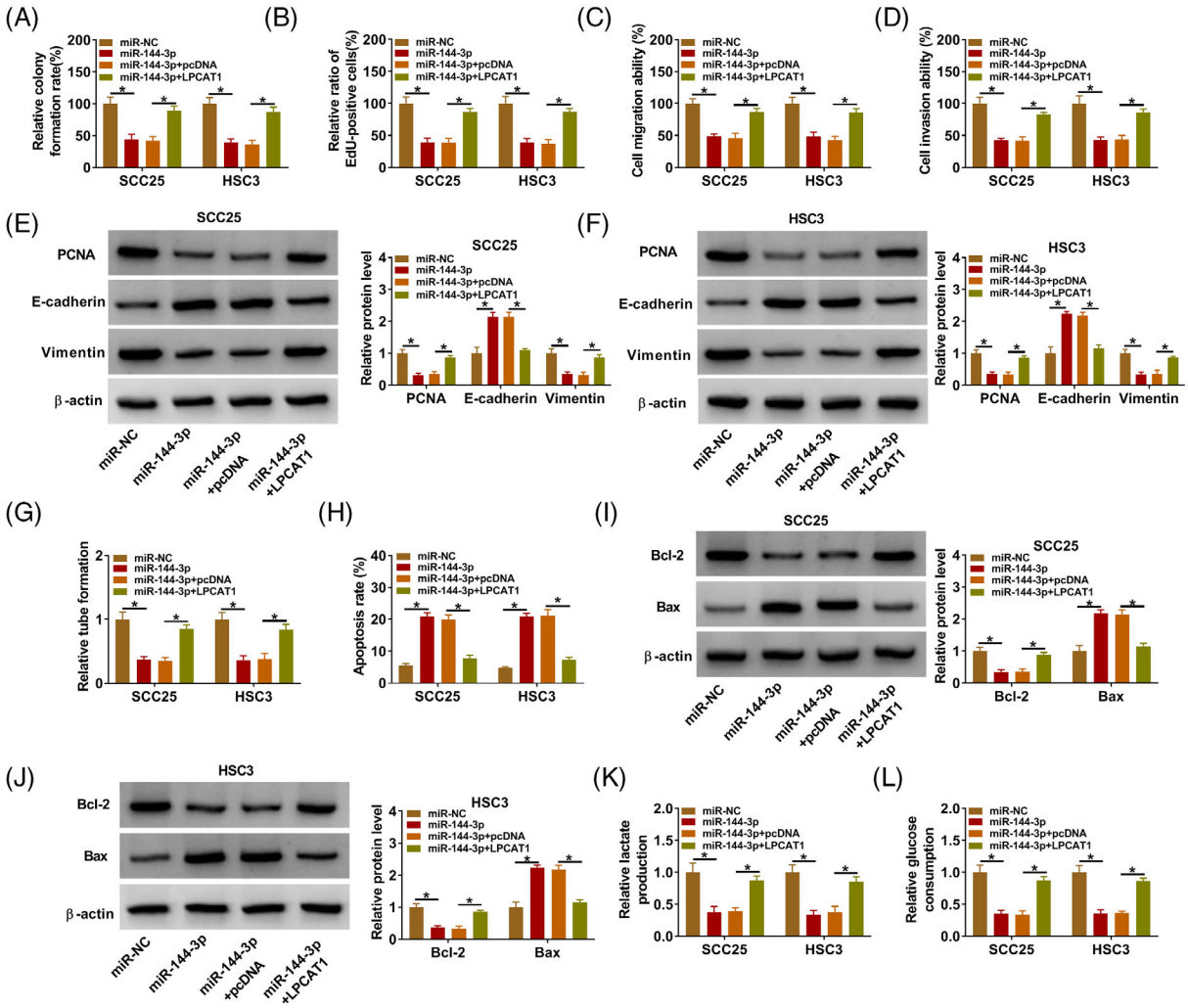

FIGURE 7 MiR-144-3p curbed proliferation, migration, invasion, angiopoiesis, and glycolysis of OSCC cells via targeting LPCAT1. (A–D) Assessment of the proliferation, migration, and invasion of OSCC cells with miR-NC, miR-144-3p, miR-144-3p+pcDNA, or miR-144-3p+LPCAT1. (E and F) Detection of protein levels of PCNA, E-cadherin, and Vimentin in the above cells. (G and H) Analysis of the angiopoiesis and apoptosis of the above cells. (I and J) Evaluation of protein levels of Bcl-2 and Bax in the above cells. (K and L) Measurement of lactate production and glucose consumption in the above cells. $^*p < .05$

performed. We discovered that miR-144-3p might target LPCAT1 (Figure 6A). Also, administration of miR-144-3p mimic decreased the luciferase activity of the LPCAT1 3′UTR WT reporter but did no effect on the LPCAT1 3′UTR MUT reporter (Figure 6B,C). Moreover, LPCAT1 was overtly enriched by the Bio-miR-144-3p WT probe but not the Bio-miR-144-3p MUT probe (Figure 6D). Furthermore, LPCAT1 mRNA and protein levels were higher in OSCC samples than the control samples (Figure 6E,F). Higher levels of LPCAT1 protein were also obtained in OSCC cells (Figure 6G). As expected, the inhibitory effect of miR-144-3p mimic on LPCAT1 expression was reversed by LPCAT1 overexpression (Figure 6H). In addition, circLPAR3 silencing decreased LPCAT1 expression, but this decrease was overturned by miR-144-3p inhibition (Figure 6I). These results exhibited that circLPAR3 regulated LPCAT1 expression through functioning as a miR-144-3p sponge.

3.7 | MiR-144-3p repressed proliferation, migration, invasion, angiopoiesis, and glycolysis of OSCC cells via targeting LPCAT1

Whether miR-144-3p mediates OSCC cell malignant behaviors via negatively regulating LPCAT1 expression was further investigated. The results exhibited that miR-144-3p mimic repressed cell proliferation, migration, and invasion, but these effects were whittled after LPCAT1 overexpression (Figure 7A–D). Exogenetic expression of miR-144-3p increased E-cadherin protein levels and repressed PCNA and Vimentin protein levels, but these changes were reversed by LPCAT1 upregulation (Figure 7E,F). In addition, miR-144-3p overexpression restrained angiopoiesis, induced apoptosis, elevated Bax protein levels, and decreased Bcl-2 protein levels, while these alterations were overturned by exogenous expression of LPCAT1 (Figure 7G–J). In addition, overexpression of LPCAT1 weakened the decrease in lactate production and glucose consumption in OSCC cells mediated by miR-144-3p upregulation (Figure 7K,L). In sum, miR-144-3p exerted an anti-tumor activity though targeting LPCAT1 in OSCC.

3.8 | CircLPAR3 silencing repressed OSCC growth in vivo

SCC25 cells carrying sh-circLPAR3#2 were inoculated into nude mice to investigate the function of circLPAR3 in OSCC in vivo. The results of subcutaneous tumorigenesis experiments showed that the circLPAR3-silencing nude mice exhibited smaller tumor volume and lighter tumor weight than the control group (Figure 8A,B). Also,

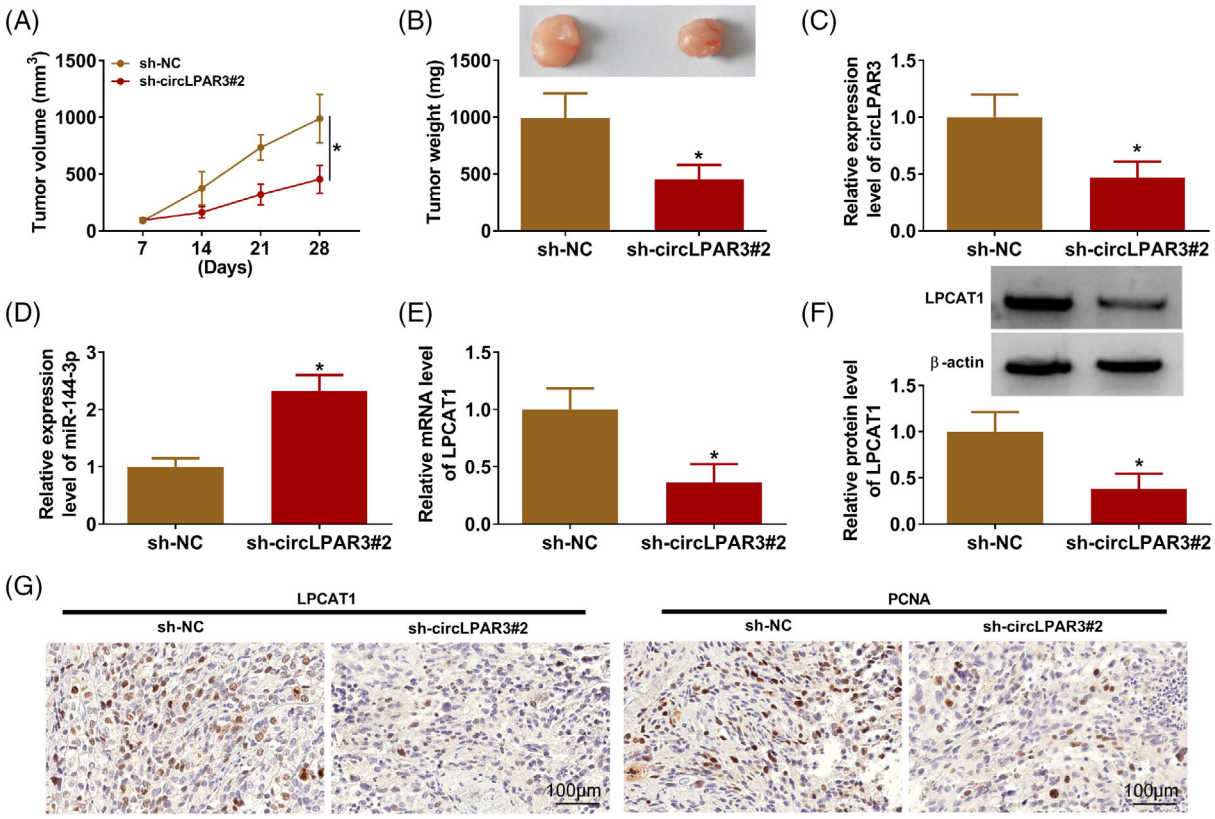

FIGURE 8 CircLPAR3 promoted OSCC growth in vivo. (A) The tumor growth curves of sh-NC and sh-circLPAR3#2 groups. (B) Representative images of xenograft tumors and the average tumor weight in sh-NC and sh-circLPAR3#2 groups. (C–F) Relative levels of circLPAR3, miR-44-3p, LPCAT1 mRNA, and LPCAT1 protein in tumor samples from sh-NC and sh-circLPAR3#2 groups. (G) IHC analysis of the number of LPCAT1/PCNA-positive cells in tumor samples from sh-NC and sh-circLPAR3#2 groups. *$p < .05$

SCC25 cells carrying sh-circLPAR3#2-derived xenograft tumors had lower levels of circLPAR3 and LPCAT1, as well as higher levels of miR-144-3p than the control group (Figure 8C–F). IHC staining showed that the number of LPCAT1/PCNA-positive cells was less in the circLPAR3-knockdown group than that in the control group (Figure 8G). Taken together, the above results suggested that circLPAR3 silencing reduced OSCC growth in vivo.

4 | DISCUSSION

The current study highlighted the regulatory action of the circLPAR3/miR-144-3p/LPCAT1 axis in OSCC advancement and increased our knowledge of the tumor-promoting function of circLPAR3.

Recent studies have uncovered the oncogenic of circLPAR3 in several tumors. Researchers reported that circLPAR3 exerted a tumor-promoting impact through upregulating MET via binding to miR-198 in ovarian cancer[22] and esophageal squamous cell cancer.[23] Cheng et al. indicated that circLPAR3 sponged miR-433/miR-375 and elevated HMGB1 expression, resulting in ESCC growth.[24] Fu et al. suggested that circLPAR3 was overexpressed in OSCC samples and cell lines, and circLPAR3 silencing decreased xenograft tumor growth and facilitated cell apoptosis, restrained cell proliferation, stemness, and migration through repressing HMGB2 by liberating miR-643.[19] Consistent with the results of Fu et al., our data exhibited that circLPAR3 had higher levels in OSCC samples and cell lines, and circLPAR3 downregulation reduced xenograft tumor growth in vivo and induced cell apoptosis, repressed cell proliferation, and reduced migration in OSCC cells in vitro. In addition, we also discovered that circLPAR3 could distinguish between OSCC samples and normal samples, and OSCC patients with high circLPAR3 expression had a worse prognosis. Furthermore, our findings exhibited that circLPAR3 silencing decreased cell invasion, angiopoiesis, and glycolysis in OSCC cells. These results highlighted the diagnostic, prognostic, and therapeutic importance of circLPAR3 in OSCC tumorigenesis.

Cytoplasmic circRNAs can absorb miRNAs to modulate gene expression in carcinogenesis.[25] Intriguingly, we discovered that circLPAR3 could facilitate OSCC cell proliferation, migration, invasion, angiopoiesis, and glycolysis through sequestering miR-144-3p and elevating LPCAT1 expression.

It has been reported that miR-144-3p plays an anti-tumor activity in many human tumors such as cervical cancer,[26] pediatric Wilms' tumor,[27] lung cancer,[28] glioblastoma,[29] and esophageal squamous cell cancer.[30] In OSCC-related studies, miR-144-3p had lower levels in OSCC samples and cells, and miR-144-3p overexpression restrained OSCC cell malignant behaviors through targeting EZH2[31,32] or ERO1L.[33] In this study, miR-144-3p was also underexpressed in OSCC samples and cells, and the sponge ability of circLPAR3 to miR-144-3p was validated by luciferase and RNA pull-down experiments. Moreover, miR-144-3p knockdown partly overturned the repressive impacts of circLPAR3 silencing on OSCC cell proliferation, migration, invasion, angiopoiesis, and glycolysis, suggesting that circLPAR3 mediated OSCC progression through interacting with miR-144-3p.

LPCAT1, a cytosolic enzyme, catalyzes the conversion of lysophosphatidylcholine into phosphatidylcholine in phospholipid metabolism.[34] Carcinogenic properties of LPCAT1 have also been described in human malignancies, such as lung adenocarcinoma[35] and castration-resistant prostate cancer.[36] A previous report showed that LPCAT1 could facilitate OSCC cell invasiveness and proliferation via increasing the biosynthesis of platelet-activating factors.[37] In addition, HOXA-AS3 promoted OSCC cell proliferation via LPCAT1.[38] Our data showed an overt elevation in LPCAT1 expression in OSCC samples and cells. LPCAT1 was then verified as a miR-144-3p target and circLPAR3 could regulate LPCAT1 expression via sponging miR-144-3p. LPCAT1 overexpression weakened miR-144-3p mimic-mediated inhibition on OSCC cell proliferation, migration, invasion, angiopoiesis, and glycolysis. These findings manifested that circLPAR3 promoted OSCC advancement via upregulating oncogene LPCAT1 through adsorbing miR-144-3p.

In summary, circLPAR3 could adsorb miR-144-3p to block the inhibiting impact of miR-144-3p on LPCAT1, leading to promoting OSCC progression. This study supports the oncogenic role of circLPAR3 in OSCC and illustrates the importance of circLPAR3 in the diagnosis, prognosis, and treatment of OSCC.

CONFLICT OF INTEREST

The authors have no conflict of interest to declare.

ORCID

Haibo Xiao https://orcid.org/0000-0002-7773-602X

REFERENCES

1. Sim YC, Hwang JH. Overall and disease-specific survival outcomes following primary surgery for oral squamous cell carcinoma: analysis of consecutive 67 patients. *J Korean Assoc Oral Maxillofac Surg*. 2019;45(2):83-90.
2. Fukumoto C, Oshima R, Sawatani Y, et al. Surveillance for patients with Oral squamous cell carcinoma after complete surgical resection as primary treatment: a single-center retrospective cohort study. *Cancers (Basel)*. 2021;13(22):5843.
3. Hakim SG, von Bialy R, Falougy M, et al. Impact of stratified resection margin classification on local tumor control and survival in patients with oral squamous cell carcinoma. *J Surg Oncol*. 2021;124(8):1284-1295.
4. Brands MT, Smeekens EAJ, Takes RP, et al. Time patterns of recurrence and second primary tumors in a large cohort of patients treated for oral cavity cancer. *Cancer Med*. 2019;8(12):5810-5819.
5. Holdt LM, Kohlmaier A, Teupser D. Molecular roles and function of circular RNAs in eukaryotic cells. *Cell Mol Life Sci*. 2018;75(6):1071-1098.
6. Suzuki H, Tsukahara T. A view of pre-mRNA splicing from RNase R resistant RNAs. *Int J Mol Sci*. 2014;15(6):9331-9342.
7. Sanger HL, Klotz G, Riesner D, Gross HJ, Kleinschmidt AK. Viroids are single-stranded covalently closed circular RNA molecules existing as highly base-paired rod-like structures. *Proc Natl Acad Sci USA*. 1976;73(11):3852-3856.
8. Jiao S, Wu S, Huang S, Liu M, Gao B. Advances in the identification of circular RNAs and research into circRNAs in human diseases. *Front Genet*. 2021;12:665233.
9. Fan HY, Jiang J, Tang YJ, Liang XH, Tang YL. CircRNAs: a new chapter in Oral squamous cell carcinoma biology. *Onco Targets Ther*. 2020;13:9071-9083.

10. Ando T, Kasamatsu A, Kawasaki K, et al. Tumor suppressive circular RNA-102450: development of a novel diagnostic procedure for lymph node metastasis from Oral cancer. *Cancers (Basel)*. 2021; 13(22):5708.
11. Liu J, Jiang X, Zou A, et al. circIGHG-induced epithelial-to-mesenchymal transition promotes Oral squamous cell carcinoma progression via miR-142-5p/IGF2BP3 signaling. *Cancer Res*. 2021;81(2):344-355.
12. Wang J, Jiang C, Li N, et al. The circEPSTI1/mir-942-5p/LTBP2 axis regulates the progression of OSCC in the background of OSF via EMT and the PI3K/Akt/mTOR pathway. *Cell Death Dis*. 2020;11(8):682.
13. Saikishore R, Velmurugan P, Ranjithkumar D, et al. The circular RNA-miRNA axis: a special RNA signature regulatory transcriptome as a potential biomarker for OSCC. *Mol Ther Nucleic Acids*. 2020;22: 352-361.
14. Li Y, Gong L, Qin N, et al. Comprehensive analysis of circRNA expression pattern and circRNA-miRNA-mRNA network in oral squamous cell carcinoma. *Oral Oncol*. 2021;121:105437.
15. Fontemaggi G, Turco C, Esposito G, di Agostino S. New molecular mechanisms and clinical impact of circRNAs in human cancer. *Cancers (Basel)*. 2021;13(13):3154.
16. Ai Y, Wu S, Zou C, Wei H. Circular RNA circFOXO3 regulates KDM2A by targeting miR-214 to promote tumor growth and metastasis in oral squamous cell carcinoma. *J Cell Mol Med*. 2021:1-11.
17. Ai Y, Tang Z, Zou C. circ_SEPT9, a newly identified circular RNA, promotes oral squamous cell carcinoma progression through miR-1225/PKN2 axis. *J Cell Mol Med*. 2020;24(22):13266-13277.
18. Shao Y, Song Y, Xu S, Li S, Zhou H. Expression profile of circular RNAs in oral squamous cell carcinoma. *Front Oncol*. 2020;10:533616.
19. Fu Y, Qiu C, Yang Y, Lu J, Qi Y. CircLPAR3 acts as an oncogene in oral squamous cell carcinoma through regulating the miR-643/HMGB2 network. *Biochem Genet*. 2021.
20. Wang Y, Guo W, Li Z, et al. Role of the EZH2/miR-200 axis in STAT3-mediated OSCC invasion. *Int J Oncol*. 2018;52(4):1149-1164.
21. Sharma S, Sandhowe-Klaverkamp R, Schlatt S. Differentiation of testis xenografts in the prepubertal marmoset depends on the sex and status of the mouse host. *Front Endocrinol (Lausanne)*. 2018;9:467.
22. Xu F, Ni M, Li J, et al. Circ0004390 promotes cell proliferation through sponging miR-198 in ovarian cancer. *Biochem Biophys Res Commun*. 2020;526(1):14-20.
23. Shi Y, Fang N. Circular RNA LPAR3 sponges microRNA-198 to facilitate esophageal cancer migration, invasion, and metastasis. *Cancer Sci*. 2020;111(8):2824-2836.
24. Cheng H, Jiang W, Song Z, et al. Circular RNA circLPAR3 facilitates esophageal squamous cell carcinoma progression through upregulating HMGB1 via sponging miR-375/miR-433. *Onco Targets Ther*. 2020;13:7759-7771.
25. Thomson DW, Dinger ME. Endogenous microRNA sponges: evidence and controversy. *Nat Rev Genet*. 2016;17(5):272-283.
26. Zhang C, Liao Y, Liu P, et al. FABP5 promotes lymph node metastasis in cervical cancer by reprogramming fatty acid metabolism. *Theranostics*. 2020;10(15):6561-6580.
27. Liu CL, Wang WH, Sun YL, et al. MiR-144-3p inhibits the proliferation and metastasis of pediatric Wilms' tumor cells by regulating Girdin. *Eur Rev Med Pharmacol Sci*. 2018;22(22):7671-7678.
28. Chen YJ, Guo YN, Shi K, et al. Down-regulation of microRNA-144-3p and its clinical value in non-small cell lung cancer: a comprehensive analysis based on microarray, miRNA-sequencing, and quantitative real-time PCR data. *Respir Res*. 2019;20(1):48.
29. Lan F, Yu H, Hu M, Xia T, Yue X. miR-144-3p exerts anti-tumor effects in glioblastoma by targeting c-met. *J Neurochem*. 2015;135(2): 274-286.
30. Wang P, Yang Z, Ye T, et al. lncTUG1/miR-144-3p affect the radiosensitivity of esophageal squamous cell carcinoma by competitively regulating c-MET. *J Exp Clin Cancer Res*. 2020;39(1):7.
31. He L, Liao L, Du L. miR-144-3p inhibits tumor cell growth and invasion in oral squamous cell carcinoma through the downregulation of the oncogenic gene, EZH2. *Int J Mol Med*. 2020;46(2):828-838.
32. Yao Y, Liu Y. LINC00662 promotes oral squamous cell carcinoma cell growth and metastasis through miR-144-3p/EZH2 axis. *Yonsei Med J*. 2021;62(7):640-649.
33. Li X, Li Y, Jiang C, Chen L, Gan N. MicroRNA-144-3p inhibits tumorigenesis of Oral squamous cell carcinoma by downregulating ERO1L. *J Cancer*. 2020;11(3):759-768.
34. Du Y, Wang Q, Zhang X, et al. Lysophosphatidylcholine acyltransferase 1 upregulation and concomitant phospholipid alterations in clear cell renal cell carcinoma. *J Exp Clin Cancer Res*. 2017; 36(1):66.
35. Wei C, Dong X, Lu H, et al. LPCAT1 promotes brain metastasis of lung adenocarcinoma by up-regulating PI3K/AKT/MYC pathway. *J Exp Clin Cancer Res*. 2019;38(1):95.
36. Han C, Yu G, Mao Y, et al. LPCAT1 enhances castration resistant prostate cancer progression via increased mRNA synthesis and PAF production. *PLoS ONE*. 2020;15(11):e0240801.
37. Shida-Sakazume T, Endo-Sakamoto Y, Unozawa M, et al. Lysophosphatidylcholine acyltransferase1 overexpression promotes oral squamous cell carcinoma progression via enhanced biosynthesis of platelet-activating factor. *PLoS ONE*. 2015;10(3):e0120143.
38. Zhao Y, Yao R. Long non-coding RNA HOXA-AS3 promotes cell proliferation of oral squamous cell carcinoma through sponging microRNA miR-218-5p. *Bioengineered*. 2021;12(1):8724-8737.

How to cite this article: Su Z, Pan C, Xie H, Ning Y, Li S, Xiao H. Downregulation of circLPAR3 inhibits tumor progression and glycolysis by liberating miR-144-3p and upregulating LPCAT1 in oral squamous cell carcinoma. *Laryngoscope Investigative Otolaryngology*. 2022;7(2):425-436. doi:10.1002/lio2.771